Multiple pathways in the trafficking and assembly of connexin 26, 32 and 43 into gap junction intercellular communication channels

Patricia E. M. Martin*,‡, Geraldine Blundell, Shoeb Ahmad, Rachel J. Errington and W. Howard Evans‡

Department of Medical Biochemistry, University of Wales College of Medicine, Heath Park, Cardiff CF14 4XN, UK

*Present address: Department of Radiology, Wales Heart Research Institute, University of Wales College of Medicine, Heath Park, Cardiff CF14 4XN, UK

‡Authors for correspondence (e-mail: martinpe@cf.ac.uk)

Accepted 24 July 2001

Journal of Cell Science 114, 3845-3855 (2001) © The Company of Biologists Ltd

SUMMARY

The assembly of gap junctions was investigated in mammalian cells expressing connexin (Cx) 26, 32 and 43 fused to green, yellow or cyan fluorescent proteins (GFP, YFP, CFP). Targeting of Cx32-CFP and 43-GFP to gap junctions and gap junctional communication was inhibited in cells treated with Brefeldin A, a drug that disassembles the Golgi. However gap junctions constructed of Cx26-GFP were only minimally affected by Brefeldin A. Nocodazole, a microtubule disruptor, had little effect on the assembly of Cx43-GFP gap junctions, but perturbed assembly of Cx26-GFP gap junctions. Co-expression of Cx26-YFP and Cx32-CFP in cells treated with Brefeldin A resulted in assembly of gap junctions constructed of Cx26-YFP. Two amino acids that distinguish Cx26 from Cx32 in transmembrane domains were mutated in Cx32 to investigate underlying mechanisms determining trafficking routes to gap junctions. One mutation, Cx32I28L, conferred on it partial Cx26-like trafficking properties as well the post-translational membrane insertion characteristics of Cx26, suggesting that a key determinant regulating trafficking was present in the first transmembrane domain. The results provide a protein trafficking basis for specifying and regulating connexin composition of gap junctions and thus selectivity of intercellular signaling, with Cx32 and 43 trafficking through the secretory pathway and Cx26 also following an alternative pathway.

Key words: Connexin-fluorescent protein chimera, Gap junction, Trafficking pathways.

INTRODUCTION

Plasma membrane proteins are generally trafficked from the ER to the cell surface via the secretory pathway. Connexins (Cx), the subunit proteins of gap junction communication channels are thought to progress along this canonical pathway during which oligomerisation into hexameric connexon hemichannels occurs (Evans et al., 1999; Musil and Goodenough, 1991; Yeager et al., 1998), a process occurring concurrently or soon after co-translational folding during protein insertion into the endoplasmic reticulum (Diez et al., 1999; Falk et al., 1997).

Gap junctions are ubiquitous intercellular channels underpinning direct cell to cell communication and tissue integration (Kumar and Gilula, 1996). About 20 different connexins have been identified in mammalian genomic maps. All connexins are believed to maintain a common topography in the membrane with four transmembrane domains, cytoplasmic N- and C-termini, and one intracellular and two extracellular loops. Connexins vary mainly in the amino acid sequences in the cytoplasmic intracellular loop and the carboxyl tail with the length of the latter varying from 16 amino acids in the nonphosphorylated Cx26 to 156 amino acids in hyperphosphorylated Cx43. The docking of hexameric connexons generates a channel that transfers cytoplasmic ions and molecules <1200 Da across the intercellular gap at cell-cell contact regions. (Nicholson et al., 2000; Bukauskas et al., 2000).

Multiple determinants govern connexin oligomerisation, which may result in the formation of homo or heteromeric connexons. This is an area of intense interest, especially since mutations detected in connexin communicationopathies such as Charcot-Marie Tooth X-linked disease, sensori-neural deafness and skin abnormalities appear to influence connexin trafficking and their assembly into gap junction channels (Deschenes et al., 1997; Martin et al., 1999; Martin et al., 2000a; Martin and Evans, 2000; VanSlyke et al., 2000; Castro et al., 1999). Connexins are characterised by rapid turnover rates (half-lives of 1-4 hours) (Laing and Beyer, 2000; Laird et al., 1995). The synthesis and breakdown of gap junctions are complex processes influenced by hormones that can induce a rapid increase in gap junction expression, especially those constructed predominantly if not exclusively of Cx26 (e.g. in breast during lactation) (Monaghan et al., 1994; Locke et al., 2000), and in livers subject to hormonal activation (Kojima et al., 1994; Kojima et al., 1996). In Cx32-knockout mice, the circadian expression of Cx26 and acute phase responses are not influenced by abolishing Cx32 expression (Temme et al., 2000). These results in tissues co-expressing Cx32 and Cx26 suggest that the presence of independent gap junction assembly pathways can provide a mechanism that accounts for such disparate expression profiles. Cx26 has previously been shown

to have different intracellular trafficking properties to Cx43 and Cx32 on the basis of subcellular distribution studies in guinea pig liver (Diez et al., 1999) and by biochemical and photometric analysis using connexin-aequorin chimerae (George et al., 1999). The present work further analyses the trafficking properties of connexins by use of Cx26, Cx32 or 43-fluorescent protein chimerae and point mutations in TM1 and TM4 that distinguish between Cx26 and Cx32. Cx26, 32 and Cx43-GFP chimerae were shown previously to be of the predicted molecular weight when expressed in COS-7 or HeLa cells (Martin et al., 2000b). These chimeric connexins were targeted to gap junctions that transferred Lucifer yellow and electrical current and they also propagated intercellular Ca^{2+} waves (Paemeleire et al., 2000). In the present work we have examined in real time using single and dual channel visualisation the delivery of fluorescently tagged connexins to gap junctions in cells in which either Golgi or microtubule functions were disrupted. Furthermore we have identified an amino acid determinant in the first transmembrane domain of Cx32 that, when mutated, resulted in its transformation into a connexin showing Cx26-like trafficking and membrane insertion properties (i.e. relative insensitivity of gap junction assembly to Golgi disruption and redistribution by Brefeldin A (BFA)) and high dependence of trafficking on microtubular integrity. The dual trafficking properties of connexins can explain the independent generation of gap junctions under specific physiological and developmental situations, especially those constructed of Cx26. Since gap junctions assembled from different connexins demonstrate a range of channel selectivity properties, the presence of multiple assembly pathways provides a further mechanism for cells to rapidly remodel the composition gap junctions and thus how they function as direct intercellular signaling networks.

MATERIALS AND METHODS

Construction of chimeric Cx-FP cDNA

To create constructs Cx26, 32 and 43-GFP, the open reading frame of the relevant Cx cDNA was amplified from plasmids containing the cDNA using primers containing *Bgl*II (for Cx26 and Cx43) or *Hin*dIII (for Cx32) restriction enzyme sites to ensure inframe fusion with the amino terminus of enhanced-GFP (eGFP) in the vector pe-GFP-N1 (Clontech) (Martin et al., 2000b; Paemeleire et al., 2000). With Cx26-YFP and Cx32-CFP chimerae, the relevant Cx was isolated from the GFP chimeric construct by restriction enzyme digestion such that the Cx cDNA was fused in frame to the relevant FP vector (*Bgl*II for Cx26 and *Hin*dIII for Cx32) followed by direct ligation of Cx26 into the *Bgl*II site of pe-YFP-N1 and of Cx32 into the *Hin*dIII site of vector pe-CFP-N1 (Clontech) and subsequent transformation into *E. coli* (DH5α) (Gibco-BRL). Positive clones were identified by miniplasmid preparation and restriction enzyme analysis. In attempts to generate a functional Cx43 red fluorescent protein (Cx43-rFP), Cx43 was also fused in frame to the N-terminus of pDsRed-N1 (Clontech) using the procedure outlined above.

Site directed mutagenesis

Two point mutations were introduced into the first and fourth transmembrane domains of Cx32 at positions I28 and V206, respectively. The amino acids were converted to those found in Cx26, namely, 28L and 206I, using the Stratagene Quickchange site directed mutagenesis kit according to manufacturer's instructions. This procedure is based on a one step PCR reaction using overlapping primers containing the base pair change. The primers used were as follows and the mutated codon is underlined:

Cx32I28L forward primer 5′: GTA TGG CTG TCC GTC CTC TTT ATC TTC AGA ATC

Cx32I28L reverse primer: 5′ GAT TCT GAA GAT AAA GAG GAC GGA CAG CCA TAC

Cx32V206I forward primer: 5′CTG CAT TAT CCT CAA CAT CGC GGA GGT GGT GTA

Cx32V206I reverse primer: 5′ G TAC ACC ACC TCC GCG ATG TTC AGG ATA ATG CAG

PCR products were directly transformed into competent *E. coli* (XL-Blue) and several colonies were selected and sequenced. Colonies with the correct base change and no erroneous mutations were selected for subsequent study.

Expression of Cx-FP proteins in HeLa and COS-7 cells

HeLa Ohio cells (ECACC, UK) were selected to express Cx26-GFP or Cx43-GFP on the basis of their sensitivity to Geneticin (G418-sulphate 4 mg/ml) and selection by FACS as previously described (Martin et al., 2000b; Paemeleire et al., 2000). Cell populations selected for the GFP chimerae were maintained in Dulbecco's modified Eagles medium, supplemented with 10% fetal calf serum, penicillin/streptomycin (100 μg/ml), amphotericin (100 μg/ml) and L-glutamine (2 mM) and geneticin). Stocks of cells were split 1:10 once a week and were used for up to 10 passages.

For analysis of Cx43-rFP, Cx32-CFP, Cx26-YFP, Cx32I28L and Cx32V206I expression, COS-7 cells (5×10^5) were plated onto 25 mm^2 coverglass chambers (GibcoBRL) and transfected with 0.5 μg of the relevant cDNA using Lipafectamine 2000 reagent (GibcoBRL) as per manufacturer's instructions. For co-expression analysis of Cx32-CFP and Cx26-YFP, cells were transfected with 1 μg and 0.5 μg of DNA respectively to account for the sensitivity of detection of the CFP chromophore. Expression was analysed 24-48 hours post transfection.

Immunolocalisation of connexin-GFP proteins

Cells (1×10^5) were cultured on 16 mm^2 coverslips overnight and fixed the next day in 4% formaldehyde and processed for immunocytochemical analysis as described (Martin et al., 1998). To study the cellular localisation of connexins incorporating the two site-specific mutations, cells were stained with Gap34R, a rabbit polyclonal antibody generated against the carboxyl tail of Cx32 (Martin et al., 2000a). For analysis of changes to the cytoskeleton following drug treatments, a monoclonal antibody to p58 (Sigma, 1:100 dilution) was used to determine the position of the ERGIC; for microtubules, an rabbit polyclonal antibody to β-tubulin (Sigma; 1:100 dilution) was used. In each case, goat anti-rabbit or goat anti-mouse IgG conjugated to Cy3 was used as the secondary antibody. For actin, TRITC-labelled Phalloidin (Sigma; 0.5 μg/ml) was used. Cells were mounted in fluorsave (Calbiochem) prior to viewing on a Zeiss Axiovert 100 microscope.

The effect of BFA on cells co-transfected with Cx32-CFP and Cx26-YFP was analysed in live cells viewed on an Axiovert 100 microscope linked to a Hamamatsu digital camera system at ex 480/30 and em 515LP for YFP and GFP; at ex 436/20 and em 480/40 for CFP; and cells were excited at 540-550 nm and viewed at 580-590 nm for Cy3 and DsRed.

Functionality of chimeric and mutant Cx constructs

Confluent monolayers of HeLa cells selected to express Cx43 or Cx26-GFP constructs were microinjected with Lucifer yellow CH $Li2^+$ salt (LY, 5% w/v in 0.3 M LiCl). Fifteen minutes later, cells were fixed in 4% formaldehyde, and viewed on a Zeiss Axiostat microscope using filter sets 05 (395-440 nm/460-470 nm) to determine the number of cells transferring dye. In these selected cell populations, functionality was calculated as the percentage of cells transferring dye to two or more neighbouring cells. Eighteen hours prior to

experiments, protein expression was enhanced by addition to the medium of 5 mM sodium butyrate (George et al., 1998a).

The functionality of wild-type (wt) Cx32 and mutant Cx32I28L was determined by a procedure in which the cDNA (250 μg/ml) was microinjected into the nucleus of every cell in a colony (up to 20 cells) of contiguous HeLa cells, followed 24 hours later by microinjection of Lucifer yellow as described above (George et al., 1998a). Functionality in these small colonies of cells was calculated as the percentage of cells transferring dye to two or more neighbouring cells. In studies of differences in functionality between drug treated and control cells, statistical significance was calculated by a Student's *t*-test analysis. $P<0.05$ was considered significant.

Drug treatments

Cells were treated with the following drugs dissolved in culture media; 5 μg/ml BFA to disrupt the Golgi; 20 μg/ml nocodazole (Noc) to disrupt the microtubules; 1 μg/ml cytochalasin D to depolymerise actin filaments. Exposure of cells to drugs was for 5-6 hours prior to the Lucifer yellow or fluorescent imaging experiments. Cells were also incubated at 15°C in media for 6 hours to monitor intracellular trafficking of Cx43-GFP or Cx26-GFP.

Time-lapse microscopy and image analysis

Cells (5×10^5) were cultured on 22 mm^2 round coverslips and mounted in a chamber containing cDMEM and the relevant traffick-disrupting drug and viewed under an Axiovert 100 microscope attached to a BioRad MRC 1024MP laser scanning system.

Time-lapse sequences were acquired using a ×40 1.3 oil immersion lens typically resulting in an xyt series with the following parameters: (collection interval 30 seconds, cycle 5.86 seconds and sequence length 60 seconds). To quantify Cx-GFP movement, three vesicular time points were compared at 30 seconds (t1) (Fig. 1A), 15 minutes (t2) (Fig. 1B) and at 30 minutes (t3) (Fig. 1C). The temporal co-localisation coefficients were extracted and henceforth termed the mobility coefficient (C_E). This value describes the amount of red fluorescent pixels (at 30 seconds) overlapping or colocalising with blue fluorescent pixels (at 30 minutes). If the value tended towards 1 then the extent of overlap was 100%, indicating no movement. If the value tended towards 0 then the extent of overlap was minimal and vesicular movement has occurred. The extent of temporal overlap is represented on a pixel-by-pixel basis by a scatter plot, showing the distribution at t1 (red axis) compared with t3 (blue axis). Complete colocalisation is shown along the line of identity (Fig. 1E). Scattering away from this line reflects a degree of mobility (Fig. 1E). This approach is analogous to that used to measure spatial co-localisation as previously described (Manders et al., 1993). Images were collected with a look-up table, which avoided clipping of signal pixel intensity between 0-10 and 245-255 in the areas of interest. Background was defined from a similar area each time and subtracted before calculating the coefficient value. For co-localisation, all the signal above background was considered apart from saturated fluorescence (245-255 nm), contributed mainly by connexin reservoirs located intracellularly, which were excluded from the analysis. The results are expressed as the mean coefficient±s.e.m. from three cell sets under the various conditions described above and repeated on three separate occasions. Statistical significance was calculated using a Student's *t*-test analysis; $P<0.1$ was considered significant.

Co- and post-translational integration of connexins into membranes

Cell free synthesis of Cx32 containing mutations I28L and V206I (see above) was carried out as previously described (Ahmad et al., 1999). Briefly, the relevant cDNA was transcribed and translated in vitro using the coupled reticulocyte lysate transcription/translation system (TNT Quick, Promega) in the presence of ^{35}S-labelled (15 μCi) methionine and cysteine (Promix, Amersham). To study co-translational membrane integration, the reactions were set up in the presence of canine pancreatic microsomes. Glutathione (5 mM) was added to compensate for small amounts of diothiothreitol present in the Promix. On completion of protein synthesis, DNase and RNase were added and reactions continued for 30 minutes at 30°C to degrade template cDNA and its transcripts. For post-translational membrane insertion, canine microsomes were then added and the reactions were continued at 30°C for a further 90 minutes to allow presynthesised connexins to insert into membranes. Membrane-integrated connexins were separated from 'free' connexins by centrifuging the suspension (150,000 ***g*** for 90 minutes) through a 0.5 M sucrose cushion. Membrane pellets were washed by centrifugation and loosely attached proteins removed by resuspension in 0.1 M $NaCO_3$, pH 11.0 followed by recentrifugation. Pellets were then solubilised in SDS-PAGE buffer and analysed after SDS-PAGE and autoradiography.

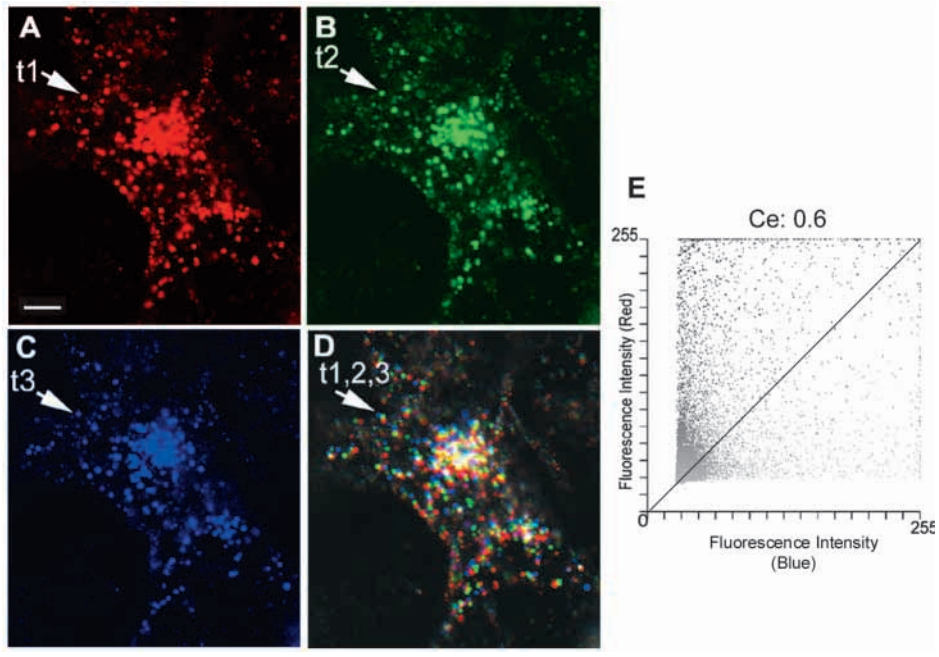

Fig. 1. Assignment of colocalisation coefficient to Cx-GFP expressing cells. Real time trafficking of Cx26-GFP was recorded every 30 seconds over a 30 minute time period. Time points 1 (30 seconds, t1), 30 (15 minutes, t2) and 60 (30 minutes, t3) were assigned red (A), green (B) and blue (C) channels, respectively. Merging the three images gives a view of the vesicular trafficking in the cell (D). (E) Representative fluorogram of the extent of colocalisation of red and blue channels where the line of identity is indicated (see Materials and Methods for details). C_e, colocalisation coefficient. Bar, 5 μm. Arrows indicate vesicular movement between the three time points.

RESULTS

Effects of disruption of the secretory pathway on gap junction communication

We have shown previously that the trafficking determinants of connexins do not reside on the cytoplasmic carboxyl tail that varies in length between different connexins, except for a short sequence proximal to TM4 (Martin et al., 2000b; Ahmad et al., 2001). Thus, trafficking to gap junctions of Cx26 containing the carboxyl tail of Cx43 or Cx32 and fused to aequorin was unaffected by BFA treatment, but was disrupted by nocodazole treatment (George et al., 1999). By contrast, Cx32 or Cx43 fused to aequorin showed trafficking properties that were disrupted by BFA treatment but were relatively insensitive to nocodazole treatment (George et al., 1999). Therefore, in the present work we examined first whether HeLa cells expressing Cx26 or Cx43 fused to GFP formed functional gap junctions before and after BFA treatment. HeLa cells were selected for these experiments because they do not endogenously express connexin proteins and are not functionally coupled by gap junctions (i.e. they do not transfer dye between each other) (Elfgang et al., 1995; George et al., 1998a). These experiments permitted dye transfer in selected cell populations to be assigned to the expression of the relevant connexin and its assembly into functional gap junctions (Fig. 2). Cells were treated with BFA for periods of up to 6 hours to allow for recruitment of connexons from intracellular stores to gap junctions, a process that occurs in 5-15 minutes as previously described (George et al., 1998a).

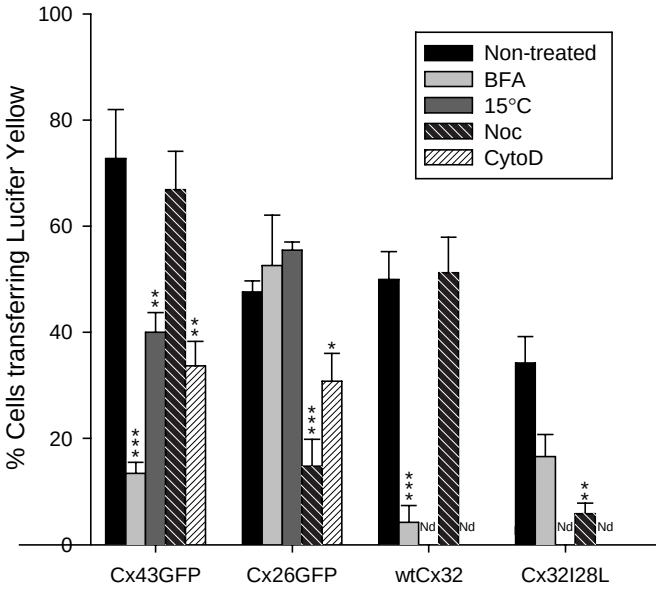

Fig. 2. The effect of inhibitors of the secretory pathway and cytoskeleton on intercellular transfer of Lucifer yellow. HeLa cells expressing the various connexin proteins were assessed for their ability to transfer Lucifer yellow across gap junctions as described in Materials and Methods. The results are expressed as the percentage of cells transferring dye to >2 neighbouring cells ±s.e.m. At least 90 cells were injected per experiment, n=3. The effect of 15°C and cytochalasin D on cells expressing wtCx32 and Cx32I28L was not determined (Nd). Statistical significance was determined by Student t-test analysis. P<0.05 was considered significant. *P<0.05; **P<0.001; *** P<0.0005.

Attachment of GFP to connexins had little effect on the functionality of gap junctions. Fig. 2 shows that 72.8±9.2% of Cx43-GFP and 47.6±2.1% of Cx26-GFP-expressing HeLa cells were dye coupled. HeLa cells expressing wtCx32 were used as a control in these experiments and 50±5.2% of the cells were communication competent. Treatment of cells with BFA for periods of up to 6 hours resulted in disruption of the Golgi and its redistribution to perinuclear areas, validated by fixing and staining parallel cells with p58, a marker protein for ERGIC (Fig. 3A,B). After dispersion of the Golgi by BFA treatment, dye coupling in cells expressing Cx43-GFP or wtCx32 was significantly reduced compared with control cells 13.4±2.1% (P<0.0001) and 4.2±3.2% (P<0.0001), respectively (Fig. 2). Incubation of Cx43-GFP expressing cells at 15°C, to disrupt the efficiency of the secretory pathway (Hirchberg et al., 1998), resulted in a 46% reduction in the ability of cells to transfer Lucifer yellow, which was significantly different to control cells (P<0.001). These results show that Cx43-GFP recruitment to gap junctions was arrested by two different treatments that disrupt trafficking of proteins along the secretory pathway. By contrast, dye transfer in Cx26-GFP expressing cells was not significantly influenced by BFA treatment or by incubating cells at 15°C (P=0.25 and 0.67, respectively) (Fig. 2).

The assembly of gap junctions was also examined by image analysis using COS-7 cells co-transfected with Cx32-CFP and Cx26-YFP. Under normal conditions, both Cx32 and Cx26 were found to colocalise 24 hours post-transfection at areas of cell to cell contact (Fig. 4A-C). However, following BFA treatment, colocalisation at the plasma membrane was not observed, with Cx26-YFP found at areas of cell to cell contact and Cx32-CFP located predominantly intracellulary (Fig. 4D-F). Similar results were obtained in HeLa cells expressing Cx43-GFP or Cx26-GFP (Fig. 6), confirming that treatment of connexins with procedures that disrupt the secretory pathway have similar effects in both cell types.

Expression of Cx43-rFP was also examined in COS-7 cells. However, the chimera expressed did not target to the plasma membrane and became trapped intracellulary, suggesting that the DsRed protein is not a suitable partner for connexin proteins (data not shown). Problems in using the DsRed fluorphore as the reporting protein in trafficking studies have recently been highlighted (Baird et al., 2000).

Identification of trafficking determinants

To analyse the molecular basis accounting for the different trafficking characteristics of connexins, amino acids in the first transmembrane domain and in the fourth transmembrane domain, which differed between Cx32 and Cx26, were mutated. Mutants Cx32I28L and Cx32V206I were expressed in HeLa and COS-7 cells and their trafficking and functional properties before and after BFA treatment compared with wtCx32. Both mutants targeted efficiently to the plasma membrane (Fig. 5A). Treatment of COS-7 cells transiently expressing Cx32I28L with BFA for up to 6 hours had little effect on the targeting of the mutant connexin to the plasma membrane (Fig. 5B). By contrast, targeting of Cx32V206I was disrupted by BFA treatment in a similar manner to that of Cx32-CFP (Fig. 5C; Fig. 4D) and wtCx32 (George et al., 1999), resulting in a predominant intracellular location.

The modified trafficking characteristics observed with

Cx32I28L led us to investigate the ability of gap junctions formed by this mutated connexin to transfer Lucifer yellow before and after BFA treatment. Fig. 2 shows that Cx32I28L formed functional gap junctional channels with 35±5.8% of cells dye-coupled. Treatment of cells expressing Cx32I28L with BFA reduced the efficiency of dye transfer to 18.75±3.3%. Statistical analysis showed that this action of BFA on assembly was not as significant (P=0.25) as in cells expressing wtCx32, where dye transfer was severely compromised (P<0.0001) (Fig. 2). Thus the results suggest that I28L has lost a measure of its BFA sensitivity and become highly dependent on microtubular integrity, as shown in cells expressing Cx26GFP (see below) and wtCx26 (George et al., 1999).

Effects of disruption of the cytoskeleton on communication across gap junctions

Differences observed in the trafficking behaviour of the different connexins to the gap junction prompted a study of the role of microtubules and actin filaments on the targeting of connexins to the plasma membrane and cell coupling efficiency. Cells expressing connexins were treated with nocodazole or cytochalasin D and the functional status of their gap junctions studied. To validate the effects of the reagents and the localisation of cytoskeletal structural elements, cells were stained with antibodies to β-tubulin to study microtubule integrity, and with phalloidin for actin filaments (Fig. 3C-F). After incubation of the cells with nocodazole, microtubules were shattered as shown by the β-tubulin staining (Fig. 3C,D). Following treatment with cytochalasinD, depolymerisation of the actin filaments was evident (Fig. 3E,F).

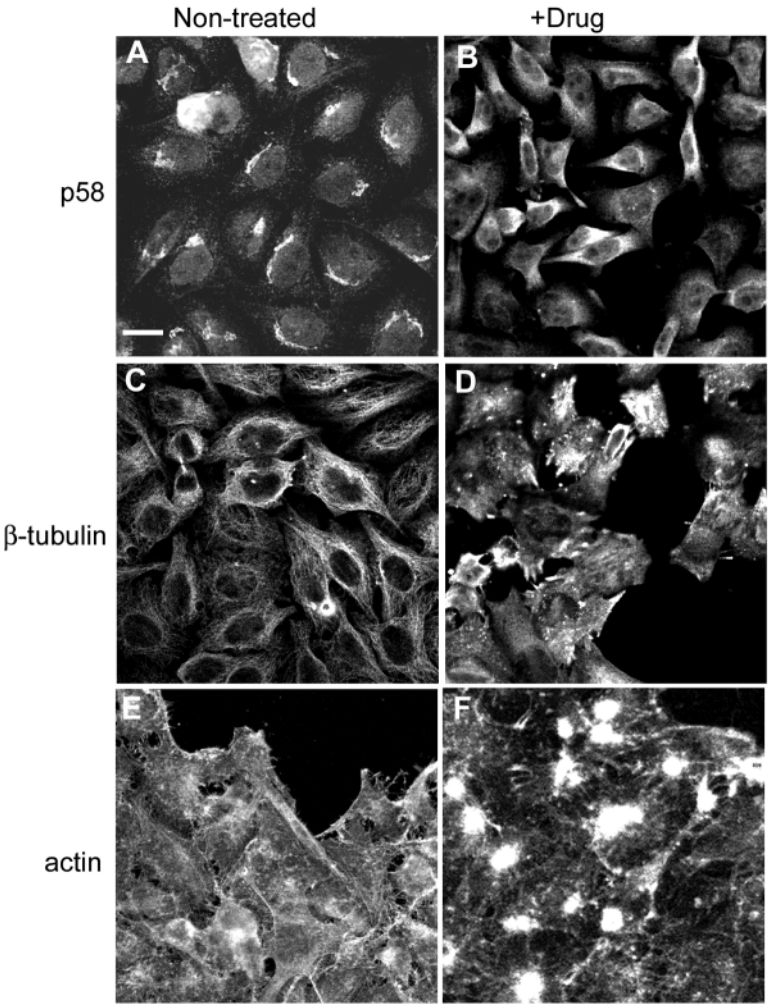

Fig. 3. The effect of Brefeldin A, Nocodazole and Cytochalasin D on Golgi, microtubules and actin filaments. Confluent monolayers of HeLa cells were fixed and stained with a primary antibody to ERGIC (p58) under control conditions (A) and following 5 hours treatment with 5 μg/ml BFA (B); microtubule integrity was monitored by use of antibodies to β-tubulin under normal conditions (C) and following 5 hours treatment with 20 μg/ml nocodazole (D). The structural integrity of actin filaments was determined by staining with pholloidin before (E) and after 5 hours treatment with 1 μg/ml cytochalasin D (F). Bar, 10 μm.

Exposure of HeLa cells expressing Cx26-GFP to nocodazole resulted in a 70% reduction in gap junctional dye coupling compared with non-treated cells (P<0.0005). Similarly, the efficiency of dye transfer in cells expressing Cx32I28L was reduced following nocodazole treatment from 35.0±5.8% to 5.2±2.6% (P<0.001) (Fig. 2). Conversely, there was no significant effect of nocodazole on the functionality of cells expressing Cx43-GFP or wtCx32, with intercellular dye transfer similar to that of untreated cells (Fig. 2). To correlate the nocadozole sensitivity of Cx32I28L and Cx26-GFP observed in dye-coupling studies, cells expressing these connexins were also immunostained to determine connexin expression following nocodazole treatment. Wild-type Cx26 or Cx26GFP plaques were rarely found at the plasma membrane following nocodozole treatment (Fig. 5D), unlike cells expressing wtCx32, which displayed gap junction plaques at points of cell to cell contact (Fig. 5E). Cells expressing Cx32I28L showed fewer gap junction plaques at the plasma membrane and an increased intracellular distribution of the protein as observed with wtCx26 (Fig. 5D,F). These results suggest that efficient targeting of newly synthesised Cx26-GFP and Cx32I28L to the plasma membrane and the assembly of gap junctions requires intact microtubules.

Disruption of actin filaments by cytochalasin D in HeLa cells resulted in a reduction of dye transfer by 50% by Cx43-GFP gap junctions and by 40% by Cx26-GFP gap junctions. However, the effects of cytochalasin D were not as marked as with BFA in cells expressing Cx43-GFP and with nocodazole in cells expressing Cx26-GFP. These results show that intact actin filaments are likely to be important for the targeting of both connexins to gap junctions.

Time-lapse microscopy

To investigate the kinetics of intracellular trafficking of various connexins and to focus on differences observed between their targeting and assembly into functional gap junctions, vesicular-like movement was monitored by time-lapse microscopy in live cells expressing Cx26-GFP or Cx43-GFP before and after drug treatment. Sequential images were recorded every 30 seconds over 30 minutes. Connexin trafficking events were measured

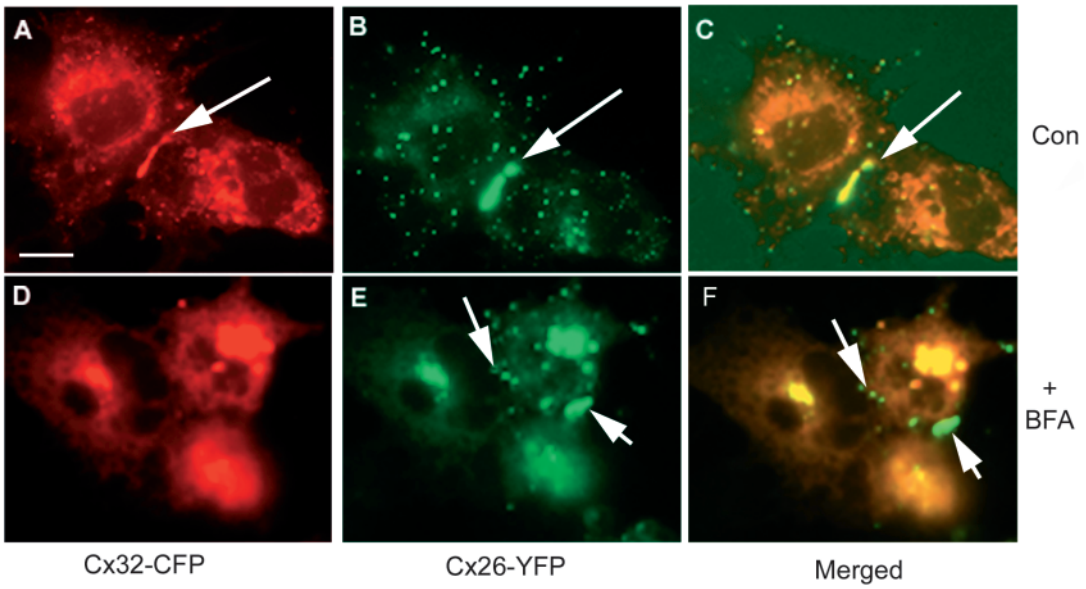

Fig. 4. The effect of BFA on Cx32-CFP and Cx26-YFP in co-transfected COS-7 cells. COS-7 cells were co-transfected with cDNA encoding Cx32-CFP and Cx26-YFP. Cells expressing both proteins were examined before and after BFA treatment. (A-C) No drug treatment. Cx32-CFP (A), Cx26-YFP (B) and merged image (C) showing colocalisation of both proteins especially at a presumed gap junction. (D-F) Cells treated with BFA for 6 hours. Cx32-CFP (D), Cx26-YFP (E) and merged image (F) showing absence of Cx32-CFP at the plasma membrane. For the purpose of image analysis CFP was assigned to the red channel and YFP to the green channel, resulting colocalisation in the merged image is yellow. Bar, 10 μm. Arrows indicate targeting to gap junctions.

at 30 second, 15 minute and 30 minute time points and each time point was assigned a colour: red, green and blue, respectively (Fig. 1). Combining or merging these three time points provided a visual description of the extent of vesicular movement over this period (Fig. 1). For example, white corresponds to no movement over the entire period, yellow corresponds to vesicular movement after 15 minutes only, and cyan indicates that movement stopped between the 30 second and 15 minute time points. As described in Materials and Methods, the mobility coefficient was extracted from the merged image and a comparison of trafficking of Cx43-GFP and Cx26-GFP in non-treated, BFA and nocodazole treated cells was carried out.

A mean mobility coefficient in untreated cells of 0.68±0.07 was determined with Cx43-GFP and 0.70±0.10 with Cx26-GFP (Fig. 1E) (Table 1). Fluorescent saltatory movement of both types of Cx-GFP-containing vesicles to the cell periphery and points of cell contact was observed as reflected in the variation in colour in the merged images (Fig. 6A,B). Cx43-GFP trafficking in cells treated with BFA was reduced

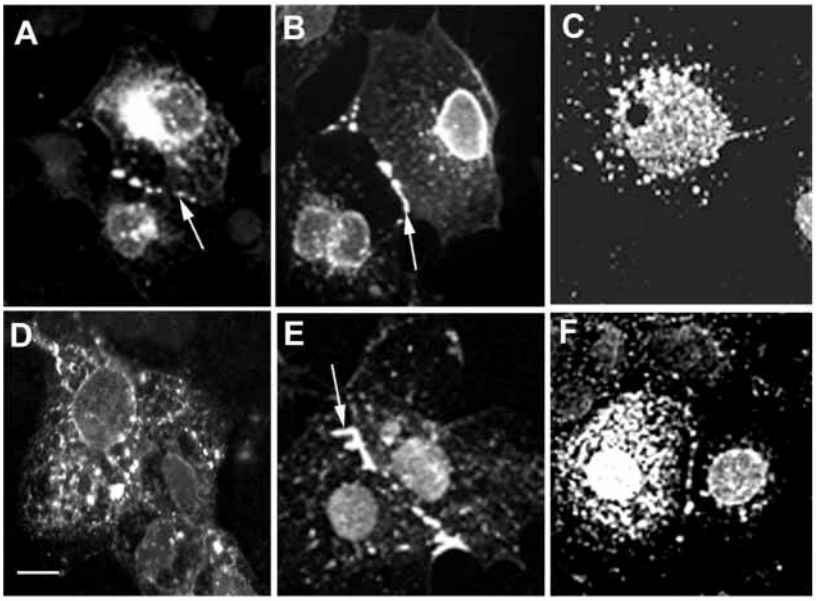

Fig. 5. The effect of BFA on the trafficking of mutant Cx32I28L. COS-7 cells were transfected with cDNA encoding Cx32I28L and 48 hours post-transfection cells were fixed and stained with an antibody against the carboxyl tail of Cx32 (Gap34R). (A) Cx32I28L under normal conditions. Similar images were obtained for wtCx32 and mutant Cx32V206I. (B) Mutant Cx32I28L 6 hours post-treatment with BFA. Arrow shows retention of gap junctions at the plasma membrane. (C) Cx32V206I 6 hours post treatment with BFA. Note that Cx32 staining was intracellular. (D) wtCx26 6 hours following nocodazole treatment showing that Cx26 was intracellular. (E) wt Cx32 6 hours following nocodazole treatment. Arrow shows gap junctions. (F) Mutant Cx32I28L 6 hours following nocdoazole treatment showing limited plasma membrane but much increased intracellular staining. D and F show a reduction in plasma membrane staining. Bar, 10 μm, Arrows indicate targeting to the gap junction. Parallel staining of the cells with p58 or β-tubulin was used to confirm that disassembly of the Golgi following BFA treatment and shattering of the microtubules following nocodazole treatment had occurred in a similar manner to that shown in Fig. 3 (not shown).

compared with the controls (Fig. 6C), especially movement to and from the plasma membrane with the mobility coefficient shifting from 0.68±0.08 to 0.93±0.002 reflecting this decrease in movement. Also, extensive white staining was seen in the merged image, especially at perinuclear regions (Fig. 6C) reflecting the redistribution of the Golgi induced by BFA treatment. However, in Cx26-GFP-expressing cells treated with BFA, the mobility coefficient was similar to that seen in untreated cells and fluorescent salutatory movement of Cx26-GFP vesicles was still observed. Further supporting the minimal effect of BFA on trafficking of Cx26-GFP was the continual arrival of new vesicles at the plasma membrane, as shown in the merged image (Fig. 6D). This data corroborates the functional dye studies, which shows that after BFA treatment Cx26-GFP cells maintain their gap junction coupling, whereas Cx43-GFP-expressing cells lose their communication properties (Fig. 2).

Treatment of cells with nocodazole caused a marked reduction in vesicular movement of Cx43-GFP and Cx26-GFP

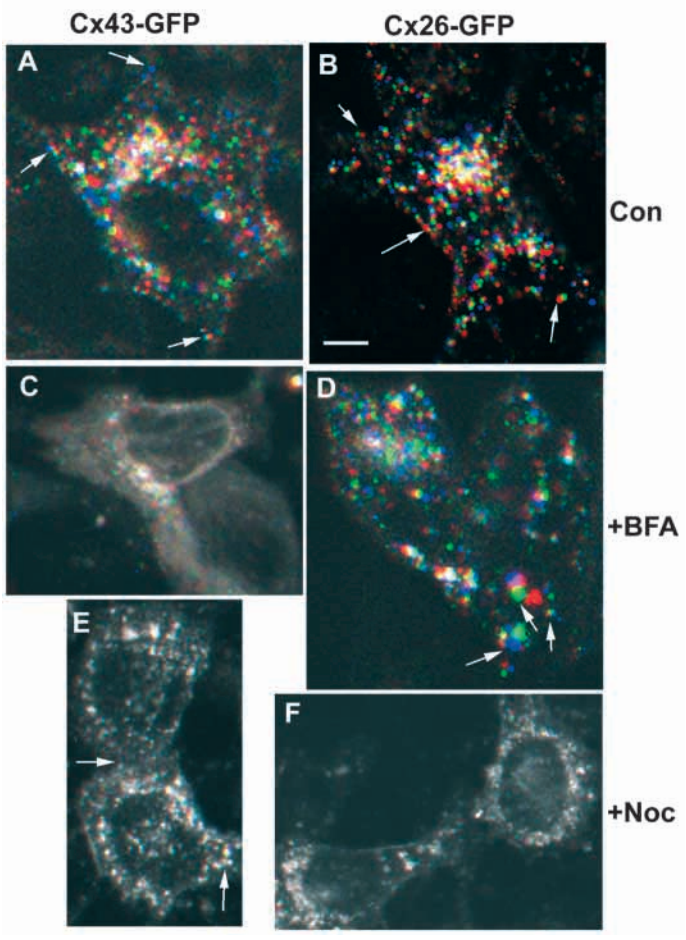

Fig. 6. The effect of BFA and nocodazole on vesicular trafficking of Cx43-GFP and Cx26-GFP. Images were analysed as described in Fig. 1 before and after treatment of the cells with BFA or nocodazole for 5 hours. Red, green and blue vesicles indicate vesicular trafficking, a white image indicates colocalisation of the three time points. Cx43-GFP (A) and Cx26-GFP (B) under normal conditions; Cx43-GFP (C) and Cx26-GFP (D) following BFA treatment; Cx43-GFP (E) and Cx26-GFP (F) following nocodazole treatment. Arrows point to gap junctions at the plasma membrane.

Table 1. Mobility co-efficients of Cx43 and Cx26-GFP before and after drug treatment

	Non-treated	+BFA	+Noc
Cx43-GFP	0.68±0.08	0.93±0.005‡	0.97±0.01*
Cx26-GFP	0.70±0.1	0.69±0.05	0.96±0.02*

The vesicular trafficking of Cx43 and Cx26-GFP studied by confocal microscopy was determined before and after drug treatment by assigning a colocalisation co-efficient that reflected the vesicular movement of the protein occurring between time points 1 (t1, 30 seconds) and 60 (t3, 30 minutes) of the experiment, as described in Materials and Methods (Fig. 1). The results represent the mean colocalisation co-efficient±s.e.m. determined from three experimental sets under the various treatments.

*P<0.1.

‡P<0.05.

in the cells with a shift in the mobility coefficients to 0.97±0.01 and 0.96±0.01 (Table 1), respectively. In cells expressing Cx26-GFP, it was notable that this decrease in mobility was associated with a reduction in plasma membrane connexin fluorescence. However, in cells expressing Cx43-GFP, although a redistribution of connexin fluorescence was evident, many vesicles were still observed near the cell periphery (Fig. 6E,F). The mobility coefficient measurements show that vesicular trafficking was significantly lower than that in untreated control cells expressing Cx43-GFP or Cx26-GFP (P<0.1). However, the continuing presence of Cx43-GFP at the plasma membrane suggested intact gap junctions, a conclusion supported by the functional dye transfer studies (Fig. 2). Again, the predominant intracellular localization of Cx26-GFP also correlated with reduced dye transfer observed in cells expressing this chimera in the presence of nocodazole (Fig. 2).

Membrane insertion properties of Cx32, Cx32I28L and Cx32V206I

Trafficking of proteins commences following their insertion into the ER. Therefore, we investigated whether the two routes followed by Cx26 and Cx32, or Cx43 to gap junctions could be distinguished at the ER level, especially since it has been

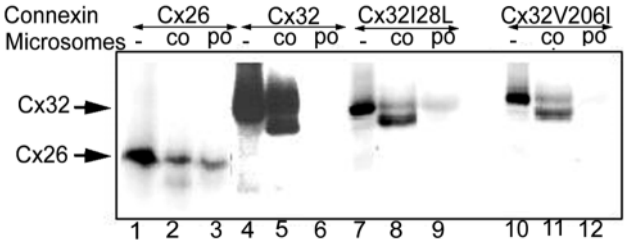

Fig. 7. Co- and post-transitional insertion of wild-type and mutated connexins into microsomal membranes. WtCx32 and Cx26, Cx32I28L or Cx32V206I were synthesised in the absence of microsomal membranes (−), or with microsomes added co-translationally (co) or post-translationally (po). For co- and post-translational studies, membranes were separated from free connexins by centrifugation through a sucrose cushion, washed in an alkaline buffer and then analysed for the presence of membrane-inserted connexins by SDS-PAGE. Lanes 1-3, Cx26; lanes 4-6, Cx32; lanes 7-9, Cx32I28L; lanes 10-12, Cx32V206I. The faster migrating bands (approx. 5 kDa less than full length connexins) are caused by abnormal proteolytic cleavage occurring in vitro due to a signal peptidase (Falk et al., 1997).

demonstrated by in vitro studies that Cx26 was inserted post-translationally in contrast to Cx32 (Ahmad et al., 1999; Zhang et al., 1996). We investigated whether the two Cx32 mutations had assumed Cx26-like membrane insertion properties. Fig. 7 shows that Cx32I28L also demonstrated post-translational insertion properties, whereas Cx32 was only inserted co-translationally. On the contrary, Cx32V206I, which maintained its Cx32 trafficking properties, was not inserted post-translationally into microsomes (Fig. 7). These results suggest that the mechanism of insertion of connexins into the ER may dictate the pathway followed in their assembly into gap junctions.

DISCUSSION

The results presented provide further evidence that multiple mechanisms operate in the assembly of connexins into gap junction intercellular communication channels. The conclusions reached stand against a background that most cells generally express more than one connexin isoform, and assemble homomeric or heteromeric connexons leading to the formation of homotypic or heterotypic gap junctions as has been demonstrated in liver (Diez et al., 1999), breast (Locke et al., 2000), lens (Jiang and Goodenough, 1996) and vascular smooth muscle cells (He et al., 1999). Channel permeability and the signalling messengers moving across gap junctions are likely to be determined by modulation of the connexin subunit composition that can dictate pore diameter and thus selectivity, as demonstrated using artificial (Elfgang et al., 1995; Cao et al., 1998); or physiological (Bevans et al., 1998; Goldberg et al., 1999; Niessen et al., 2000) substrates. The composition of gap junctional hemichannels is programmed at the connexin oligomerisation stage of biogenesis, an early event occurring in the endoplasmic reticulum-Golgi intermediate compartment (Diez et al., 1999; Falk et al., 1994; Falk et al., 1997).

We used immunocytochemistry, kinetic monitoring and multi-colour imaging of fluorescently tagged connexin movement in cells in conjunction with dye transfer across gap junctions to show that the assembly process of gap junctions constructed of Cx43 or Cx32 was different to that of gap junctions composed of Cx26. All three connexins tagged with GFP formed functional gap junctions (Paemeleire et al., 2000; Martin et al., 2000b). Similar results have also been obtained with other connexins fused at the C-terminus to fluorescent proteins (Jordan et al., 1999; Holm et al., 1999; Falk, 2000). In the present work we show that trafficking of fluorescently tagged Cx43 and 32 and their assembly into gap junctions were disrupted by BFA treatment or by lowering the ambient temperature to 15°C, procedures shown to collapse and redistribute the Golgi apparatus inside the cell (Doms et al., 1989; Peyroche et al., 1999) or reduce vesicular trafficking, respectively (Hirchberg et al., 1998). By contrast, trafficking of Cx26-GFP and its assembly into gap junctions were only reduced to a minor extent by BFA treatment and lowering the temperature, but were highly sensitive to nocodazole, a drug demonstrated to disassemble microtubules. These results extend the conclusions reached when other connexin chimerae were expressed in cells to measure intracellular Ca^{2+} cytoplasmic environments along trafficking pathways leading to gap junction assembly (George et al., 1998b; George et al., 1999; Martin et al., 1998). These studies also showed that gap junctions assembled from Cx43 and Cx32 fused to the N-terminus of aequorin were disrupted following BFA treatment and that junctions constructed of Cx26, containing the cytoplasmic tail of Cx43 fused to aequorin, failed to assemble following exposure of the cells to nocodazole. Additionally, measurements of aequorin chemiluminescent emission indicated that Cx43 and Cx32-Aeq were transferred from intracellular stores, located in Golgi environs to the cell surface in 10-15 minutes. By contrast, the Cx26-Aeq was detected at the cell surface in 5-10 minutes (George et al., 1998b). Further evidence that the intracellular routing of Cx32 and 26 was different was obtained in liver tissue by a subcellular fractionation approach. In guinea pig liver, although gap junctions are constructed of approximately equal amounts of Cx32 and Cx26, Golgi membranes were found to contain very low amounts of Cx26 relative to Cx32 (Diez et al., 1999). These results suggested that differential routes of gap junction formation exist in tissues such as liver and also emphasised that multiple assembly pathways are not merely confined to cells expressing recombinant tagged connexins. In hepatocytes derived from Cx32-knockout mice, the formation of Cx26 gap junctions was not inhibited by treatment with BFA (Spray et al., 2000), further supporting the conclusion that a different route was followed by Cx26. In agreement with the results now obtained in HeLa and COS cells, all these experimental approaches point to the different trafficking properties of Cx26 and offer a membrane trafficking basis to explain how delivery of gap junctions constructed of Cx26 is independently and temporally regulated, as shown, for example, in breast (Monaghan et al., 1994; Locke et al., 2000), liver (Kojima et al., 1994; Kojima et al., 1996) and in brain (Nadarajah et al., 1997) tissues.

Mechanisms of trafficking of connexins and their assembly into gap junction channels

The microtubule dependence and BFA independence of Cx26 assembly into gap junctions is a strong indicator that its trafficking from the ER is mechanistically different from that of the two other connexins now investigated. Time-lapse microscopy and confocal studies indicate that intracellular vesicular motion is a feature in propelling the three connexins studied to and from the cell surface and gap junctions. A number of explanations can be forwarded to account for results indicating that Cx26 and Cx43/32 follow different intracellular trafficking routes from the endoplasmic reticulum to gap junctions. The interruption of targeting of Cx43 and 32 to gap junctions by BFA treatment reinforces the key role played by Golgi in the assembly of gap junctions constructed from these connexins. Intracellular stores of Cx43 and 32 are held as connexons in the Golgi apparatus (George et al., 1999; Musil and Goodenough, 1993; Laird et al., 1995; Jordan et al., 1999). Although microtubules play a key role in ER-Golgi trafficking, the onward transfer from Golgi to gap junctions of Cx32 and Cx43 was minimally affected by nocodazole, a drug widely used to collapse microtubules. Similar effects have been reported in the assembly of Cx43 gap junctions in Novikoff cells (Paulson et al., 2000). Generally, disruption of microtubules only moderately attenuates Golgi to plasma membrane transport in fibroblasts and in some epithelial cells (Thyberg and Moskalewski, 1999; Wacker et al., 1997). This

contrasts with the situation in highly polarized cells such as neurons, where there is microtubule-based selective targeting to various plasma membrane domains (Bureck et al., 2000). The present results show that the trafficking of Cx26 was highly dependent on the maintenance of intact microtubules compared with Cx32 and 43. The assembly of Cx32 and Cx43 into gap junctions involves post-translational modifications, especially phosphorylation of amino acids located on the carboxyl tail. Cx26 is not phosphorylated nor (like all known connexins) glycosylated and these properties can fully accommodate its trafficking via a Golgi-evading but microtubule-dependent route to gap junctions. Although phosphorylation of Cx43 occurs at multiple sites, BFA treatment reduces overall Cx43 phosphorylation (Laird et al., 1995).

Several endocytic routes of entry into cells have now been described (Pelkmans et al., 2001), and the present results show that Cx26 follows a different exocytic route to the plasma membrane from the secretory pathway used by Cx32 and Cx43. Alternative exocytic trafficking pathways of numerous proteins that take into consideration non-involvement of Golgi functions have been described. For example, a high proportion of cholesterol transport from ER to plasma membrane is now recognised to occur rapidly via a Golgi-independent route (Heino et al., 2000). Interestingly, the kinetics of cholesterol movement from the ER (via a route that appears to bypass the Golgi) to the plasma membrane and the transfer of Cx26 from intracellular stores to the plasma membrane both occur in approximately 10 minutes (Smart et al., 1996; George et al., 1999). Cholesterol is also likely to play an important role in gap junction assembly (Malewicz et al., 1990). The Glut4 receptor, which is hormonally regulated, recycles from the plasma membrane to intracellular vesicles in a BFA-independent manner and this trafficking is also sensitive to microtubule disruption (Corvera and Czech, 1996; Patki et al., 2001). However, the details of these routes, which apparently have minimal Golgi implication, are unclear. Components of the exocytic and endocytic membrane trafficking apparatus feature in extensive recycling and involve subsets of functionally heterogeneous domains in the endocytic apparatus; some of these pathways are highly sensitive to drugs that perturb microtubules (Van Ijzendoorn and Hoekstra, 1999), a feature of the trafficking of Cx26 highlighted in this work. Alternatively, since the ER is a highly differentiated membrane system, there may be subcompartments physically contiguous to the plasma membrane that can allow direct transfer of connexins to the plasma membrane. Further work is necessary to distinguish between these possibilities and explain the non-involvement of the Golgi in the assembly of Cx26 gap junctions.

Determinants of gap junction trafficking and assembly

A single amino acid distinguishing Cx26 from 32 was shown to contribute to their different intracellular trafficking itineries. Mutating isoleucine 28 to leucine in TM1 of Cx32 resulted in adoption of Cx26-like trafficking behaviour (i.e. Cx32I28L targeting and assembly into gap junctions were observed despite the dispersion of the Golgi in these cells shown to occur following BFA treatment). This site-specific mutation also resulted in a change in the in vitro transcription-translation characteristics, with post-translational membrane insertion in addition to the conventional co-translational connexin insertion properties now occurring. Post-translational insertion into membranes was shown to be an unusual and characteristic property of Cx26 (Ahmad et al., 1999; Zhang et al., 1996). Although mutating a single amino acid in TM1 altered the trafficking properties of Cx32 such that they began to resemble the properties of Cx26, a single membrane-embedded amino acid is unlikely to be the sole targeting determinant of this multipass membrane protein. Leucine at position 28 in Cx26 is also present in Cx43, and this may explain the partial post-translation membrane insertion properties of Cx43 (Ahmad et al., 1999). The present results show that Cx43 trafficking and assembly were similar to that of Cx32 (i.e. they were BFA sensitive and nocodazole insensitive). However, rapid enhancement of Cx43 gap junction assembly, stimulated by cyclic AMP or LDL, was found to be unaffected by BFA but was sensitive to nocodazole, suggesting that under certain physiological conditions Cx43 may also traffic to gap junctions via a Golgi by-passing pathway (Paulson et al., 2000). Thus, Cx43 may follow both pathways, thereby adding to the complexities inherent in the assembly of heteromeric connexons.

Trafficking determinants are absent from the cytoplasmic carboxyl tail of Cx32 since most of the tail, except for a short sequence (amino acids 207-219) proximal to TM4, can be deleted without detriment to gap junction assembly and function as shown for Cx32 (Martin et al., 2000b; Castro et al., 1999). Further trafficking determinants are likely to reside in other regions of connexins, for example in TM3 (Ahmad et al., 2001). Unusual trafficking and assembly properties and post-translational modification were shown by Cx46, a connexin expressed in lens and osteoblasts (Jiang et al., 1993; Korval et al., 1997); this connexin also has a leucine at position 28. Analysis of a range of mutations dispersed at various domains that account for gap junction dysfunction in Charcot-Marie-Tooth X-linked disease and non-syndromic deafness indicates that multiple point-specific determinants result in intracellular retention and/or failure of connexins to oligomerise (Martin and Evans, 2000). Indeed, it is likely that the regulation of trafficking and targeting of multi-pass membrane proteins is often determined by more than one sequence feature. We suggest that the two pathways now demonstrated in extremis by Cx26 and Cx32 operate in parallel in cells. Trafficking itineraries are likely to be complex when different connexins that individually follow different trafficking routes oligomerise to generate heteromeric connexons. For example, the presence of low levels of Cx26 in guinea pig liver Golgi subcellular fractions may result from the oligomerisation of this connexin with Cx32 into heteromeric connexons trafficking mainly via the Golgi in which the major isoform was Cx32 (Diez et al., 1999). Cx26 gap junction plaques that are rapidly generated in hormonally perturbed livers (Kojima et al., 1994; Kojima et al., 1996) suggests that a Golgi bypassing, microtubule-dependent assembly route now described can allow a more rapid generation of Cx26 homomeric connexons and possibly homotypic gap junctions.

This work was supported in part by the Medical Research Council and a JREI grant. We thank Nathan Peacock for research assistance.

REFERENCES

Ahmad, S., Diez, J. A., George, C. H. and Evans, W. H. (1999). Synthesis and assembly of connexins in vitro into homomeric and heteromeric functional gap junction hemichannels. *Biochem. J.* **339**, 247-253.

Ahmad, S., Martin, P. E. M. and Evans, W. H. (2001). Assembly of gap junction channels. Identification of oligomeric intermediates and determinants and evidence of a role for calmodulin. *Eur. J. Biochem.* **268**, 4544-4552.

Baird, G. S., Zacharias, D. A. and Tsien, R. J. (2000). Biochemistry, mutagenesis and oligomerisation of DSRed, a red fluorescent protein from coral. *Proc. Natl. Acad. Sci. USA* **97**, 11984-11989

Bevans, C. G., Kordel, M., Rhee, S. K. and Harris, A. L. (1998). Isoform composition of connexin channels determines selectivity among second messengers and uncharged molecules. *J. Biol. Chem.* **273**, 2808-2816.

Bukauskas, F. F., Jordan, K., Bukauskiene, A., Bennett, M. V. L., Lampe, P. D., Laird, D. W. and Verselis, V. K. (2000). Clustering of connexin 43-enhanced green fluorescent protein gap junction channels and functional coupling in living cells. *Proc. Natl. Acad. Sci. USA* **97**, 2556-2561.

Bureck, M. A., Silverman, M. A. and Banker, G. (2000). The role of selective transport in neuronal protein sorting. *Neuron* **26**, 465-472.

Cao, F., Eckert, R., Elfgang, C., Nitsche, J. M., Snyder, S. A., Hulser D. F., Willecke, K. and Nicholson, B. J. (1998). A quantitiative analysis of connexin-specific permeability differences of gap junctions expressed in HeLa transfectants and *Xenopus* oocytes. *J. Cell Sci.* **111**, 31-43.

Castro, C., GomezHernandez, J. M., Silander, K. and Barrio, L. C. (1999). Altered formation of hemichannels and gap junction channels caused by C-terminal connexin-32 mutations. *J. Neurosci.* **19**, 3752-3760.

Corvera S. and Czech, M. P. (1998). Direct targets of phosphoinositide 3-kinase products in membrane traffic and signal transduction. *Trends Cell Biol.* **11**, 442-446.

Deschenes, S. M., Walcott, J. L., Wexler, T. L., Scherer, S. S. and Fischbeck, K. H. (1997). Altered trafficking of mutant connexin32. *J. Neurosci.* **17**, 9077-9084.

Diez, J. A., Ahmad, S. and Evans, W. H. (1999). Assembly of heteromeric connexons in guinea-pig liver en route to the Golgi apparatus, plasma membrane and gap junctions. *Eur. J. Biochem.* **262**, 142-148.

Doms, R. W., Russ, G. W. and Yewdell J. W. (1989). Brefeldin A redistributes resident and itinerant Golgi proteins to the endoplasmic reticulum. *J. Cell Biol.* **109**, 61-72.

Elfgang, C., Eckert, R., Lichtenberg-Frate, H., Butterweck, A., Traub, O., Klein, R. A., Hulser, D. F. and Willecke, K. (1995). Specific permeability and selective formation of gap junction channels in connexin-transfected HeLa-cells. *J. Cell Biol.* **129**, 805-817.

Evans, W. H., Ahmad, S., Diez, J., George, C. H., Kendall, J. M. and Martin, P. E. M. (1999). Trafficking pathways leading to the formation of gap junctions. *Novartis Found. Symp.* **219**, 44-54.

Falk, M. M. (2000). Connexin-specific distribution within gap junctions revealed in living cells. *J. Cell Sci.* **113**, 4109-4120.

Falk, M. M., Kumar, N. M. and Gilula, N. B. (1994). Membrane insertion of gap junction connexins - polytopic channel-forming membrane-proteins. *J. Cell Biol.* **127**, 343-354.

Falk, M. M., Buehler, L. K., Kumar, N. M. and Gilula, N. B. (1997). Cell-free synthesis and assembly of connexins into functional gap junction membrane channels. *EMBO J.* **16**, 2703-2716.

George, C. H., Martin, P. E. M. and Evans, W. H. (1998a). Rapid determination of gap junction formation using HeLa cells microinjected with cDNAs encoding wild-type and chimeric connexins. *Biochem. Biophys. Res. Commun.* **247**, 785-789.

George, C. H., Kendall, J. M., Campbell, A. K. and Evans, W. H. (1998b). Connexin-aequorin chimerae report cytoplasmic calcium environments along trafficking pathways leading to gap junction biogenesis in living COS-7 cells. *J. Biol. Chem.* **273**, 29822-29829.

George, C. H., Kendall, J. M. and Evans, W. H. (1999). Intracellular trafficking pathways in the assembly of connexins into gap junctions. *J. Biol. Chem.* **274**, 8678-8685.

Goldberg, G. S., Lampe, P. D. and Nicholson, B. J. (1999). Selective transfer of endogenous metabolites through gap junctions composed of different connexins. *Nat. Cell Biol.* **1**, 457-459.

He, D. S., Jiang, J. X., Taffet, S. M. and Burt, J. (1999). Formation of heteromeric gap junction channels by connexins 40 and 43 in vascular smooth muscle cells. *Proc. Natl. Acad. Sci. USA* **96**, 6495-6500.

Heino, S., Lusa, S., Somerharju, P., Ehnholm, C., Olkkonen, V. M. and Ikonen, E. (2000). Dissecting the role of the Golgi complex and lipid rafts in biosynthetic transport of cholesterol to cell surfaces. *Proc. Natl. Acad. Sci. USA* **97**, 8378-8380.

Hirchberg, K., Miller, C. M., Ellenberg, J., Presley, J. F., Siggia, E. D., Plair, R. D. and Lippincott-Schwartz, J. (1998). Kinetic analysis of secretory proteins traffic and characterisation of Golgi to plasma membrane transport intermediates in living cells. *J. Cell. Biol.* **143**, 1485-1503.

Holm, I., Mikhaliov, A., Jillson, T. and Rose, B. (1999). Dynamics of gap junctions observed in living cells with connexin43-GFP chimeric protein. *Eur. J. Cell. Biol.* **78**, 856-866.

Jiang, J. X. and Goodenough, D. A. (1996). Heteromeric connexons in lens gap junction channels. *Proc. Natl. Acad. Sci. USA* **93**, 1287-1291.

Jiang, J. X., Paul, D. L. and Goodenough, D. A. (1993). Posttranslational phosphorylation of lens fiber connexin46 - a slow occurrence. *Invest. Ophthalmol. Vis. Sci.* **34**, 3558-3565.

Jordan, K., Solan, J. L., Dominguez, M., Sia, M., Hand, A., Lampe, P. D. and Laird, D. W. (1999). Trafficking, assembly, and function of a connexin 43-green fluorescent protein chimera in live mammalian cells. *Mol. Biol. Cell* **10**, 2033-2050.

Kojima, T., Sawada, N., Oyamada, M., Chiba, H., Isomura, H. and Mori, M. (1994). Rapid appearance of connexin 26-positive gap-junctions in centrilobular hepatocytes without induction of messenger-RNA and protein-synthesis in isolated-perfused liver of female rat. *J. Cell Sci.* **107**, 3579-3590.

Kojima, T., Yamamoto, M., Tobioka, H., Mizuguchi, T., Mitaka, T. and Mochizuki, Y. (1996). Changes in cellular-distribution of connexin-32 and connexin-26 during formation of gap-junctions in primary cultures of rat hepatocytes. *Exp. Cell Res.* **223**, 314-326.

Korval, M., Harley, J. E., Hick, E. and Steinberg, T. H. (1997). Connexin46 is retained as monomers in a trans-Golgi compartment of osteoblastic cells. *J. Cell Biol.* **137**, 846-857.

Kumar, N. M. and Gilula, N. B. (1996). The gap junction communication channel. *Cell* **84**, 381-388.

Laing, J. G. and Beyer, E. C. (2000). Degradation of gap junctions and connexins. *Curr. Topics Memb.* **49**, 461-481.

Laird, D. W., Castillo, M. and Kasptzak, L. (1995). Gap junction turnover, intracellular trafficking and phosphorylation of connexin 43 in Brefeldin A-treated mammary turnover cells. *J. Cell Biol.* **131**, 1193-1203.

Locke, D., Perusinghe, N., Newman, T., Jayatilake, H., Evans, W. H. and Monaghan, P. (2000). Developmental expression and assembly of connexins into homomeric and heteromeric gap junction hemichannels in the mouse mammary gland. *J. Cell Physiol.* **183**, 228-237.

Malewicz, B., Kumar V. V., Johnson, R. G. and Baumann, W. J. (1990). Lipids in gap junction assembly and function. *Lipids* **25**, 419-427.

Manders, E. M., Verbeek, F. J. and Aten, J. A. (1993). Measurement of colocalisation of objects in dual-colour confocal microscopy. *J. Microscopy* **169**, 375-382

Martin, P. E. M and Evans, W. H. (2000). Trafficking and targeting to gap junctions of connexin 32 mutations to gap junctions in Charcot-Marie-Tooth X-linked disease. *Curr. Top. Membr.* **49**, 461-481.

Martin, P. E. M., George, C. H., Castro, C., Kendall, J. M., Capel, J., Campbell, A. K., Revilla, A., Barrio, L. C. and Evans, W. H. (1998). Assembly of chimeric connexin-aequorin proteins into functional gap junction channels. Reporting intracellular and plasma membrane calcium environments. *J. Biol. Chem.* **273**, 1719-1726.

Martin, P. E. M., Coleman, S. L., Casalotti, S. O., Forge, A. and Evans, W. H. (1999). Properties of connexin 26 gap junctional proteins derived from mutations associated with non-syndromal hereditary deafness. *Hum. Mol. Genet.* **8**, 2369-2376.

Martin, P. E. M., Archer, D., Mambetisaeva, E. T., George, C. H. and Evans, W. H. (2000a). Analysis of gap junction assembly using mutated connexins detected in Charcot Marie Tooth X-linked disease. *J. Neurochem.* **74**, 711-720.

Martin, P. E. M., Steggles, J., Wilson, C., Ahmad, S. and Evans, W. H. (2000b). Targeting motifs and functional parameters governing the assembly of connexins into gap junctions. *Biochem. J.* **349**, 281-287.

Monaghan, P., Perusinghe, N., Carlile, G. and Evans, W. H. (1994). Rapid modulation of gap junction expression in mouse mammary-gland during pregnancy, lactation, and involution. *J. Histochem. Cytochem.* **42**, 931-938.

Musil, L. S. and Goodenough, D. A. (1991). Biochemical-analysis of connexin43 intracellular-transport, phosphorylation, and assembly into gap junctional plaques. *J. Cell Biol.* **115**, 1357-1374.

Musil, L. S. and Goodenough, D. A. (1993). Multisubunit assembly of an

integral plasma-membrane channel protein, gap junction connexin43, occurs after exit from the ER. *Cell* **74**, 1065-1077.

Nadarajah, B., Jones, A. M., Evans, W. H. and Parnavelas, J. G. (1997). Differential expression of connexins during neocortical development and neuronal circuit formation. *J. Neurosci.* **17**, 3096-3111.

Nicholson, B. J., Weber, P. A., Cao, F., Chang, H., Lampe, P. and Goldberg, G. (2000). The molecular basis of selective permeability of connexins is complex and includes both size and charge. *Braz. J. Med. Biol. Res.* **33**, 369-378

Niessen, H., Harz, H., Bedner, P., Kramer, K. and Willecke, K. (2000). Selective pemeability of different connexin channels to the second messenger inositol 1, 4, 5 - trisphosphate. *J. Cell Sci.* **113**, 1365-1372.

Paemeleire, K., Martin, P. E. M., Coleman, S. L., Fogerty, K. E., Carrington, W. A., Leybaert, L., Tuft, R. A., Evans, W. H. and Sanderson, M. J. (2000). Intercellular calcium waves in HeLa cells expressing GFP-labelled connexin 43, 32 or 26. *Mol. Biol. Cell* **11**, 815-827.

Patki, V., Buxton, J., Chawla, A., Lifshitz, L., Fogarty, K., Carrington, W., Tuft, R. and Corvera, S. (2001). Insulin action on GLUT4 traffic visualised in single 3T3-L1 adipocytes by using ultra-fast microscopy. *Mol. Biol. Cel.* **12**, 129-141.

Paulson, A., Lampe, P. D., Meyer, R. A., TenBroek, E., Atikinson, M. M., Walseth, T. and Johnson, R. (2000). Cyclic AMP and LDL trigger a rapid enhancement in gap junction assembly through a stimulation of connexin trafficking. *J. Cell. Sci.* **113**, 3037-3049.

Pelkmans, L., Kartenbach, J. and Helenius, A. (2001). Caveolar endocytosis of simian virus 40 reveals a new two-step vesicular pathway to the ER. *Nat. Cell Biol.* **3**, 473-483.

Peyroche, A., Antonny, B., Robineau, S., Acker, J., Cherfils, J. and Jackson, C. L. (1999). Brefeldin A acts to stabilise an abortive ARF-GDP-Sec7 domain protein complex: involvement of specific residues of the SEC7 domain. *Mol. Cell* **3**, 275-285.

Smart, E. J., Ying, Y. S., Donzell, W. C. and Anderson, R. G. (1996). A role for caveolin in transport of cholesterol from endoplasmic reticulum to plasma membrane. *J. Biol. Chem.* **271**, 29427-29435.

Spray, D. C., Kojima, T., Scemes, E., Suadicani, S. O., Gao, Y., Zhaw, S. and Fort, A. (2000). Negative physiology: what connexin-deficient mice reveal about functional roles of individual gap junction proteins. *Curr. Top. Membr.* **49**, 509-534.

Temme, A., Ott, T., Haberberger, T., Traub, O. and Willicke, K. (2000). Acute phase response and circadian expression of connexin 26 are not altered in connexin 32-deficient mouse liver. *Cell Tissue Res.* **300**, 111-117.

Thyberg, J. and Moskalewski, S. (1999). Role of microtubules in the organisation of the Golgi complex. *Exp. Cell Res.* **246**, 263-279.

Van Ijzendoorn, S. C. and Hoekstra, D. (1999). The subapical compartment; a novel sorting centre? *Trends Cell Biol.* **4**, 144-149.

VanSlyke, J. K., Deschenes, S. M. and Musil, L. S. (2000). Intracellular transport, assembly and degradation of wild-type and disease linked mutant gap junction proteins. *Mol. Cell Biol.* **11**, 1933-1946.

Wacker, I., Kaether, C., Kromer, A., Migala, A., Almers, W. and Gerdes, H. H. (1997). Microtubule-dependent transport of secretory vesicles visualised in real time with a GFP-tagged secretory protein. *J. Cell Sci.* **110**, 1453-1463.

Yaeger, M., Unger, V. M. and Falk, M. M. (1998). Synthesis, assembly and structure of gap junction intercellular channels. *Curr. Opin. Struct. Biol.* **8**, 517-524.

Zhang, J. T., Chen, M., Foote, C. I. and Nicholson, B. M. (1996). Membrane integration of in vitro - translated gap junctional proteins: co- and post translational mechanisms. *Mol. Biol. Cell* **7**, 471-482.